The bovine uterine fluid proteome is more impacted by the stage of the estrous cycle than the proximity of the ovulating ovary in the periconception period

Coline Mahé, Paulo Marcelo, Guillaume Tsikis, Daniel Tomas, Valérie Labas, Marie Saint-Dizier

Revised

The bovine uterine fluid proteome is more impacted by the stage of the estrous cycle than the proximity of the ovulating ovary in the periconception period

Coline Mahé[1*], Paulo Marcelo[2], Guillaume Tsikis[1], Daniel Tomas[3], Valérie Labas[3], Marie Saint-Dizier[1]

[1]CNRS, IFCE, INRAE, Université de Tours, PRC, 37380, Nouzilly, France
[2]Plateforme d'Ingénierie Cellulaire & Analyses des protéines ICAP, FR CNRS 3085 ICP, Université de Picardie Jules Verne, Amiens, France
[3]INRAE, Université de Tours, CHU de Tours, Plateforme de Phénotypage par Imagerie in/eX vivo de l'ANImal à la Molécule (PIXANIM), 37380, Nouzilly, France
[*]Corresponding author: coline.mahe@inrae.fr

Abstract

Uterine secretions provide a suitable environment for sperm-selective migration during a couple of days preceding ovulation and for early embryo development before implantation. Our goal was to identify and quantify proteins in the bovine uterine fluid during the periovulatory period of the estrous cycle. Genital tracts with normal morphology were collected from adult cyclic *Bos taurus* females in a local slaughterhouse and classified into preovulatory or postovulatory stages of cycle (around days 19-21 and 0-5 of cycle, respectively; n=8 cows per stage) based on ovarian morphology. Proteins from uterine fluid collected from the utero-tubal junction to the base of each horn (four pools of two cows per condition) were analyzed by nanoLiquid Chromatography coupled with tandem Mass Spectrometry (nanoLC-MS/MS). A total of 1,214 proteins were identified, of which 91% were shared between all conditions. Overall, 57% of proteins were predicted to be secreted and 17% were previously reported in uterine extracellular vesicles. Paired comparisons between uterine horns ipsilateral and contralateral to ovulation evidenced 12 differentially abundant proteins, including five at pre-ovulatory stage. Furthermore, 35 proteins differed in abundance between pre- and post-ovulatory stages, including 21 in the ipsilateral side of ovulation. Functional analysis of identified proteins demonstrated roles in binding, metabolism, cellular detoxification and the immune response. This study provides a valuable database of uterine proteins for functional studies on sperm physiology and early embryo development.

Keywords: contralateral, ipsilateral, post-ovulatory, pre-ovulatory, proteomic, uterine fluid

Abbreviations

Contra	Contralateral horn
DAPs	Differentially abundant proteins
EVs	Extracellular vesicles
GO	Gene ontology
Ipsi	Ipsilateral horn
NanoLC-MS/MS	nanoLiquid Chromatography coupled with tandem Mass Spectrometry
NWS	Normalized weighted spectra
UF	Uterine fluid

1 Introduction

After insemination or mating in cattle, spermatozoa interact with uterine secretions and these interactions typically occur during estrus in the pre-ovulatory period of the estrous cycle. After ovulation and fertilization, the developing embryo starts to develop in the oviduct and enters the uterine horn ipsilateral to ovulation around the morula stage, at 4 to 5 days after ovulation [1]. Thus, in a short period of time ranging from 2 days before to 5 days after ovulation, spermatozoa and embryo are in direct contact with the uterine fluid (UF). The UF is a complex mixture of lipids [2], metabolites [3], amino acids [4] and proteins [5-7]. *In vitro* studies in mammals evidenced various effects of the UF on mammalian sperm and early embryos [8-11]. In cattle, incubation of spermatozoa with UF from the follicular and luteal phases resulted in higher sperm viability and motility compared to controls without fluid [8]. Uterine flushes promoted sperm capacitation *in vitro* in humans [9] but decreased sperm viability, motility and acrosome integrity in pigs [10]. The addition of low concentrations of oviductal fluid and UF in culture media supported the development of *in vitro* produced bovine embryos [11]. There is evidence that proteins secreted in the female genital tract interact with spermatozoa and embryo. For instance in humans, cystatin 3 secreted in UF has been shown to interact with spermatozoa and to promote their motility without inducing premature capacitation [12]. After *in vitro* incubation with oviduct fluid, the early bovine embryo was shown to internalize dozens of proteins crossing the zona pellucida as early as the 4- to 6-cell stage [13].

Spatiotemporal changes in the UF composition are expected to address the sequential requirements for sperm motility and selective migration, elimination of sperm in excess, and blastocyst differentiation during the periovulatory period. We previously demonstrated the dynamic changes in the oviduct fluid proteome occurring between the pre- and post-ovulatory stages of cycle in cattle [14]. Other studies in mares [5,15] and ewes [16] observed alterations of the UF proteome between the follicular and luteal phases of cycle. Moreover, the proximity of the ovulatory ovary may impact the proteome of the UF. In heifers, differences in the endometrial transcriptome between uterine horns ipsilateral and contralateral to the corpus luteum were evidenced on days 5 to 16 of cycle [17]. Although there are some proteomic reports on the UF during the luteal phase of cycle [18] and at the time of implantation [19,20] in cattle, there is currently no data in the periovulatory period. Therefore, the objective of this study was to quantitatively analyze the UF proteome in both uterine horns at pre- and post-ovulatory stages of the cycle.

2 Materials and methods

2.1 Collection of bovine uterine fluids and sample preparation

Genital tracts including the cervix, uterine horns, oviducts and ovaries from adult cyclic *Bos taurus* females were collected at a local slaughterhouse (Vendôme, France), immediately placed on ice and transported to the laboratory within two hours after animal death. Only macroscopically normal tracts with no sign of cyst, inflammation or infection were used in this study. Tracts were classified as pre-ovulatory or post-ovulatory based on ovarian morphology. Pre-ovulatory tracts contained one pre-ovulatory follicle between 11 and 20 mm in diameter and one *corpus albicans* from the previous cycle (Pre-ov; approximately days 19 to 21 of cycle). Post-ovulatory tracts displayed one *corpus hemorrhagicum* less than 0.5 cm in diameter (Post-ov; approximately days 1 to 5 of cycle). Uterine horns ipsilateral and contralateral to the side of ovulation (pre-ovulatory follicle or early corpus luteum) were cut at their base (just before the uterine body) and flushed from the utero-tubal junction with 2 mL of cold filtered phosphate buffered saline. Each uterine horn was then opened longitudinally and examined for sign of inflammation. The uterus presenting anatomical anomaly, bleeding or signs of inflammation were excluded. Cells and cellular debris were discarded from the flushing by two successive centrifugations (2000 × *g* for 10 min then 12000 × *g* for 10 min at 4°C) and UF were stored at -80°C in 2 mL polypropylene tubes. In order to reach enough protein content, pools of two cows per side × stage condition were constituted. All UF samples were thawed on ice and pools of UF were made by mixing 400 µL of each sample. In the following, the term "sample" refers to a pool of two UF. In total, four biological replicates per condition were constituted, resulting in a total of 16 UF samples. The UF samples were concentrated 2 to 4 times by centrifugation for 1 h at 12000 × *g* at 4°C in Vivaspin units (Sartorius, Stonehouse, United Kingdom) with a molecular weight cut-off of 3-kDa. Final protein concentrations of UFs ranged between 0.7 and 2.5 mg/mL (Uptima BC Assay kit, Interchim, Montluçon, France). To assess sample quality, 5 µg of proteins per UF were migrated on 4-20% SDS-PAGE precast gels for 10 min at 80 V and 30 min at 180 V (Bio-Rad, California, United States) followed by Coomassie Blue staining (ThermoFisher, Massachusetts, United States) (see Fig. S1). Then, 50 µg of proteins per UF sample were dried in 1.5 mL polypropylene tubes using a SpeedVac system (SPD 1010-230, ThermoSavant Electronic, France) and stored at -80°C before proteomic analysis.

2.2. Nanoliquid chromatography coupled with tandem mass spectrometry (nanoLC-MS/MS)

For proteomic analysis, 50 µg of protein were resuspended in 50 mM ammonium bicarbonate. Reduction and alkylation were performed by successive incubation at final concentration of 5 mM dithiothréitol in 50 mM ammonium bicarbonate (30 min at 56°C) then at a final concentration of 12.5 mM iodoacetamide in 50 mM ammonium bicarbonate (30 min at room temperature in the dark). Samples were then Trypsin/Lys-C (Promega, USA) digested with 0.01% ProteaseMAX (V2072, Promega, USA) overnight at 37°C with a ratio enzyme:substrate of 1:40. The tryptic peptide solutions were dried by vacuum centrifuge and reconstituted in 20 µL water/1% formic acid (v/v). All digested peptide mixtures were separated by on-line nanoLC and analyzed by nano-electrospray tandem mass spectrometry. The experiments were performed on an Ultimate 3000 RSLC system coupled with an Orbitrap Fusion mass spectrometer (ThermoFisher Scientific San Jose, CA, USA). The peptide mixtures were injected onto a nanotrap column (Acclaim C18, 100 µm i.d. x 2 cm length) with a flow of 5 $\mu L.min^{-1}$ and subsequently gradient eluted with a flow of 300 $nL.min^{-1}$ in an Easy-Spray column (Acclaim PepMap RSLC C18, 2 µm, 100 A, 75 µm x 50 cm) from 4 to 40% acetonitrile/0.1% formic acid (v/v) for 140 minutes. Full MS scans were acquired at high resolution (FWMH 120,000) in the Orbitrap analyzer (mass-to-charge ratio (m/z): 400 to 2000), while collision-induced dissociation (CID) spectra were recorded. The mass spectrometer was operated in positive mode in a data-dependent mode to automatically switch between orbitrap-MS and linear trap MS/MS (MS2) acquisition for 3 seconds between master scans.

2.3. Protein identification and validation

Protein identification was performed using the Mascot search engine (version 2.7; Matrix Science, London, UK) via the Proteome Discoverer software (version 2.5, Thermo Fisher Scientific) against the Uniprot *Bos taurus* database (January 2022; 23,844 sequences). Precursor mass range of 350 –5000 Da and signal-to-noise ratio of 1.5 were the criteria used for generation of peak lists. The parameters used for database searches included trypsin as enzyme, N-terminal acetylation on protein, carbamidomethylcysteine and methionine oxidation as dynamic modifications. Ion tolerance was set at 10 ppm for parent and 0.8 Da for fragment ion matches. Proteins with at least two unique peptides (False Discovery Rate (FDR) < 0.01 %) were considered. Threshold probability for peptide and protein identification were set to 95.0 % as specified by the Peptide Prophet algorithm [21] and the Protein Prophet algorithm [22].

2.4. Prediction of secretory pathways of identified proteins

Venn diagrams were built using the accession number on the jvenn tool online (http://jvenn.toulouse.inra.fr/app/example.html) [23]. Prediction of secretory pathways (presence of a signal peptide or unconventional secretion) was carried out using the Outcyte online tool (version 1.0 ; http://www.outcyte.com/) [24] and FASTA sequences as input. To confirm the presence of a signal peptide, FASTA sequences were also submitted to the SignalP online tool in Eukarya (version 6.0; http://www.cbs.dtu.dk/services/SignalP/) [25]. The gene list corresponding to identified proteins was compared to those previously reported in bovine UF-derived extracellular vesicles (EVs) [26].

2.5. Protein quantification

Proteins were quantified by a label-free approach using the spectral counting quantitative method of the Scaffold Q+ software (version 5.0.1, Proteome Software, Portland,USA, www.proteomesoftware.com). Protein abundance was then assessed in normalized weighted spectra (NWS) after normalization, as previously described [14]. Briefly, the "weighted" option is based on the assignment of each peptide to a weight according to whether they are shared or not. The normalization of spectra among the samples was realized by adjusting the sum of the selected quantitative values for all proteins within each sample to a common value, which was the average of the sums of all samples present in the experiment. This was achieved by applying a scaling factor for each sample to each protein or protein group.

2.6. Statistical analysis of data

Statistical analysis on proteins quantified with a minimum of 2.0 NWS (mean value of biological replicates) in at least one condition was performed using the Rstudio software (version 1.4.1106). Principal component analysis of all biological replicates was performed using the FactoMineR package. Protein abundance between sides in a given stage and between stages in a given side were compared by Student *t*-tests. Proteins with a t-test p-value ≤ 0.05 and a fold change ratio ≥ 1.5 were considered as differentially abundant proteins (DAPs).

2.7. Functional analysis of proteins

The gene symbols corresponding to all identified proteins were used for gene ontology (GO) membership analysis. The GO analysis was performed for molecular functions and biological processes containing "reproduction", "sperm", "embryo", "blastocyst" or "uterus" using the online Metascape tool and the *Homo sapiens* database [27]. Furthermore, the gene symbols of

DAPs between stages in the ipsilateral horn were used to build Proteomaps online based on the Kyoto Encyclopedia of Genes and Genomes (KEGG) Pathways and using the post-ovulatory:pre-ovulatory fold-change ratios as quantitative data (http://bionic-vis.biologie.uni-greifswald.de/) [28]. In the Proteomaps, functionally related proteins are arranged in polygon aeras representing the mean abundance at the pre-ovulatory stage of cycle.

3. Results

3.1. Proteins identified in the uterine fluid and secretory pathways

A total of 1,214 proteins were identified in the bovine UF, of which 91% (1,010/1,214) were shared between all conditions (Fig. 1; see the complete list of proteins in Table S1). Proteins identified in only one condition displayed very low quantitative value (< 1 NWS). Among the identified proteins, 20% (243/1,214) were predicted to contain a signal peptide and to be classically secreted, while 28% (338/1,214) were predicted to be secreted via unconventional pathways (Fig. 2 and Table S1). In addition, 17% of identified proteins (204/1,214) were previously reported in bovine UF-derived EVs [26]. Overall, 57% (686/1,214) of the identified proteins were predicted to be secreted.

3.2. Differentially abundant proteins between horns and stages

A total of 324 proteins were retained for quantitative analysis (NWS >2; Table S1). The most abundant proteins included albumin (ALB), complement proteins (C3, CFB), myosin 9 (MYH9), mucin 5B, heat shock protein 90AA1 (HSP90AA1), enolase 1 (ENO1) and annexins A1 and A2 (ANXA1, 2; see the top-15 most abundant proteins in Fig. 3). Principal component analysis (Fig. 4) of quantified proteins did not show any clear discrimination between samples, although mean values of samples at pre- and post-ovulatory clustered together on the two first principal dimensions (colored squares in Fig. 4). Paired comparisons between ipsilateral and contralateral horns evidenced 12 DAPs, i.e. 4% of quantified proteins, with fold-change ratios between 1.5 and 12.1 (Fig. 5; see quantitative values and fold-change ratios in Table S2). Furthermore, 35 proteins, i.e. 11% of quantified proteins, differed in abundance between pre- and post-ovulatory stages with fold-change ratios between 1.5 and 6.9. Of those DAPs, 21 were identified in the ipsilateral side of ovulation (Fig. 6A and 6B; Table S2).

3.3. Functional analysis of identified and differentially abundant proteins

The Metascape GO analysis of all identified proteins showed a significant enrichment in molecular functions related to binding (cadherin binding, actin binding, unfolded protein binding and protein domain specific binding) and enzymatic activities (enzyme inhibitor activity, pyrophosphatase activity, ligase activity, peptidase activity; Fig. 7A and Table S3). Among the biological processes, UF proteins were overrepresented in several metabolic processes such as peptide metabolic process, nucleobase-containing small molecule metabolic process and carbohydrate metabolic process, among others, as well as in cellular detoxification, regulation of cell morphogenesis, protein catabolic process and response to wounding (Fig. 7B). Finally, the most enriched cellular components included secretory granules lumen, vacuolar lumen, focal adhesions and the proteasome complex (Fig. 7C).

A total of 157 proteins were associated with GO terms containing “sexual reproduction”, “sperm”, “embryo”, “blastocyst” or “uterus” (see the lists of GO terms and proteins in Table S4). The DAPs associated with those terms are highlighted in Fig. 6-7. Finally, the Proteomaps in Fig. 8 shows that the DAPs between pre- and post-ovulatory stages in the horn ipsilateral to ovulation were involved in various KEGG pathways, including metabolism (SAO, LDHB, SLC9A3R1) and vesicular transport through exosomes (KRT18, CAND1).

4. Discussion

Using high-resolution mass spectrometry, this work provides a first analysis of proteins present in the bovine UF in the periovulatory period, i.e. at the time of sperm migration toward the site of fertilization and early embryo development. Overall, 91% of proteins were shared between all conditions, indicating very few specific proteins according to the proximity of the ovulatory ovary (preovulatory follicle or early corpus luteum), at least during the periovulatory period. Furthermore, most proteins detected in only one condition displayed very low quantitative values, suggesting that they were probably present but not detected due to a lack of sensitivity. Overall, 324 proteins could be quantified, which represented 21% of identified proteins. Previous proteomic analyses of the bovine UF evidenced 1,737 proteins, of which almost all could be quantified [6], while in another study, 699 proteins were identified but only 235 (34%)

could be quantified [29]. Different quantitative approaches and sensitivity of the mass spectrometer may partly explain these discrepancies between studies.

The UF were analyzed without albumin elimination to avoid loss of proteins bound to albumin and because albumin has reported roles in sperm physiology [30-32] and participates in the bioavailability of steroid hormone in the uterus [33]. However, albumin was by far the most abundant protein, quantified three times more than all other proteins; its signal probably hindered those of other proteins. Albumin was also found in high abundance in other proteomic studies in bovine [20] and ovine [16] UF. Albumin was identified as one of the main acceptors of cholesterol during bull sperm capacitation [30] and is commonly used in *in vitro* fertilization media [31]. In humans, albumin promotes H+ efflux, one of the steps of capacitation, by interacting with its channels on sperm [32].

Overall, only 4% of proteins differed in abundance between both uterine horns. This result is in accordance with a previous proteomic study in which the proximity of the corpus luteum had no effect on uterine protein abundance on either day 7 or 15 of cycle in cows [18]. Accordingly, no difference between the ipsilateral and contralateral horns were found for metabolites [34] and amino acids [4] in the bovine UF. However, a transcriptomic study discovered 217 differentially expressed genes between ipsilateral and contralateral horns at day 5 post-estrus in synchronized heifers [17]. Taken together, these data suggest that synthesized proteins may differ in abundance inside luminal epithelial cells but not in the secretions. In cyclic cows, the contractile activity and tonicity of the uterus reaches a maximum during estrus [35], and this probably contributes to the intensive mix of proteins in the two uterine horns during this period. In the present study, the stage of the cycle had three times more effect than the side on protein abundance (11% of DAPs). In another proteomic study in cattle, 24% (40/167) of proteins differed in abundance between day 7 (early luteal phase) and day 15 (late luteal phase) of cycle [18]. In ewes, 39% of proteins were differentially abundant between estrus and the luteal phases of cycle [16]. Here, we compared stages very close in time, ranging from around 3 days before to 4-5 days after ovulation, which may explain the relatively low impact of the ovulatory stage on protein abundance.

Proteins identified in the periovulatory UF were enriched in GO terms related to the regulation of cell morphogenesis and protein catabolic process, including cathepsins (CTSB, D, F) and cysteine-rich proteins like CRIP2. This is in agreement with the fact that the endometrium is vastly remodeled during the periovulatory period and displays high rates of cell proliferation

and apoptosis compared to the mid and late luteal phases [36]. CRIP2 has been identified as one secreted protein playing a role in endometrial remodeling in pigs [37]. In pigs and sheep, several cathepsins have also been reported to take part in endometrial renewal [38,39]. The identified proteins were also involved in a large panel of metabolic processes, including carbohydrate and cellular amino acid metabolism. In cattle during the early luteal phase (day 4 to 7 of cycle), the metabolism of amino acids is related to epithelial cell proliferation and the periovulatory remodeling of the endometrium [40]. Moreover, carbohydrates like glucose constitute a major source of energy for sperm motility and capacitation [41,42], as well as embryo development [43]. Of interest, DAPs between stages in the ipsilateral UF were also enriched in KEGG pathways related to metabolism, including the Na(+)/H(+) exchange regulatory cofactor NHE-RF1 (SLC9A3R1), which was more abundant at pre- than at post-ovulatory stages. The abundance of SLC9A3R1 in sperm has been related to male fertility in pigs [44]. In mice, SLC9A3R1 was shown to interact with sperm ion channels and was proposed as an intermediator needed for chloride influx, one of the mechanisms of capacitation [45].

Cellular detoxification was another enriched biological process and included various peroxiredoxins (PRDX 1, 2 and 6) and thioredoxins (TXN, TXNRD1, TXNDC17), all involved in the regulation of reactive oxygen species. PRDX1 and 2 were quantified at relatively high abundance (5-6 NWS on average) in all samples. The presence of those proteins in the UF suggests a role in maintaining the redox balance and controlling excessive production of reactive oxygen species in the UF. Sperm motility and embryo development depend on low levels of reactive oxygen species [46]. Peroxiredoxins 1 and 6 have been shown to protect sperm from lipid peroxidation [47] and promote sperm motility [48] in humans. Moreover, supplementation of recombinant TXN in the bovine embryo culture medium increased blastocyst rates compared to controls [49].

In addition to protection against cell oxidative stress, proteins like serpins (SERPINA10, B1, C1, D1), peroxidases (GPX, PXDN, MPO) and DAPs more abundant at Post-ov than at Pre-ov (LGALS1, RUVBL1) have reported roles in mediating the immune response [50–53]. This is in accordance with previous proteomic studies on the bovine UF, in which various proteins involved in the immune system were also identified [18,20,54]. It is well-known that a physiological immune response takes place in the uterine lumen following the first contact with sperm [55]. Neutrophils eliminate sperm through direct cell-cell interactions and neutrophil extracellular traps (NETs), which hinder sperm motility [56]. Proteins in the periovulatory UF

are expected to modulate sperm elimination. SERPINB1, identified in all samples but at low abundance (< 2 NWS), has been shown to restrict the formation of NETs by inhibiting the activity of neutrophil elastase *in vitro* [50,51]. Furthermore, the incubation of bull sperm with myeloperoxidase (MPO), a NET-derived protein identified below the quantitative threshold in all samples, impairs the sperm membrane, acrosome integrity and lipid peroxidation [52]. Finally, recombinant galectin-1 (LGALS1) has been shown to induce the expression of anti-inflammatory interleukin-10 and the regulatory T lymphocyte marker FOXP3 in bovine endometrium [53].

Regarding the cellular components of the identified UF proteins, the focal adhesion and proteasome complex, including numerous proteins of the 26S proteasome, were overrepresented. In accordance, in mares, uterine cytobrush sampling during estrus revealed that overexpressed genes in fertile compared to subfertile mares were involved in focal adhesions [57]. Furthermore, inhibition of proteins of the 26S proteasome reduced boar sperm tyrosine phosphorylation and Zn^{2+} efflux compared to controls [58], suggesting a role for proteasome proteins secreted in the UF in sperm capacitation.

Most proteins identified in the bovine UF were enriched in binding functions, also in accordance with previous proteomic studies in cattle [20] and pigs [59]. Of interest, some of the most abundant proteins in the periovulatory UF, like annexins A1, A2 and myosin-9, were previously reported to interact with sperm [60] and embryos [13] after incubation with bovine oviduct fluid *in vitro*. Although embryos interact first with the oviduct fluid, sperm interact first with the UF, then the oviduct fluid. Further studies are needed to know with which proteins sperm interact first during their uterine migration and whether those interactions compete with further interactions in the oviduct.

Proteins in the UF may be secreted via the classical reticulum endoplasmic-Golgi pathway or in EVs [61,62], and one possible mechanism of UF protein interaction with sperm and embryos is EV-mediated. In our study, 17% of proteins were reported in bovine UF-derived EVs and some DAPs more abundant at the pre-ovulatory stage (KRT18), or in the opposite, at the post-ovulatory stage (CAND1), were enriched in vesicular transport through exosomes. Interaction of spermatozoa with uterine EVs has been reported as one mechanism allowing for the delivery of SPAM1, a hyaluronidase important for the crossing of cumulus cells in mice [63]. Uterine EVs were shown to interact with human sperm head and tail after only 15 min of co-incubation and to promote tyrosine phosphorylation [64], one sign of sperm capacitation. The uptake of

uterine EVs was also reported in the ovine embryo [65], suggesting important roles for further development.

Although providing valuable data on the uterine proteome, this study presents some limitations. Uterine fluids were collected from slaughterhouse tracts. Although tracts were transported on ice with less than two hours between animal death and collection, we cannot rule out limited changes in the protein content due to post-mortem modifications. Furthermore, in order to obtain enough protein content per sample and decrease inter-individual variability, pools of two uterine flushes at the same stage of the cycle were analyzed; this precludes any evaluation of inter-individual or inter-breed variability on the UF proteome.

In conclusion, the data reported here expand our knowledge on the environment encountered by spermatozoa after insemination and the early embryo a few days after fertilization. In contrast with our previous data on the oviduct fluid proteome [14,66], no major effect of the proximity of the ovulatory ovary on protein abundance was evidenced. Further work is now needed to understand the potential role of the DAPs between stages on the adaptative response of the uterus to allow sperm migration then early embryo development in a short time window.

Acknowledgments

The authors warmly thank Thierry Delpuech and Albert Arnoult for collecting the tracts at the slaughterhouse. This work was funded by INRAE and Agence Nationale de la Recherche under grant number ANR-18-CE92-0049.

Declarations of competing interest

The authors declare that they have no competing interests**.**

Data availability

The mass spectrometry proteomics data have been deposited to the ProteomeXchange Consortium [67] via the PRIDE (version 2.5.7) [68] partner repository with the dataset identifier PX038325.

References

[1] Hackett AJ, Durnford R, Mapletoft RJ, Marcus GJ. Location and status of embryos in the genital tract of superovulated cows 4 to 6 days after insemination. Theriogenology 1993;40:1147–53. https://doi.org/10.1016/0093-691X(93)90285-D.

[2] Simintiras CA, Sánchez JM, McDonald M, Lonergan P. Progesterone alters the bovine uterine fluid lipidome during the period of elongation. Reproduction 2019;157:399–411. https://doi.org/10.1530/REP-18-0615.

[3] Silva FACC, da Silva GF, Vieira BS, Neto AL, Rocha CC, Lo Turco EG, et al. Peri-estrus ovarian, uterine, and hormonal variables determine the uterine luminal fluid metabolome in beef heifers. Biol Reprod 2021;105:1140–53. https://doi.org/10.1093/biolre/ioab149.

[4] Hugentobler SA, Diskin MG, Leese HJ, Humpherson PG, Watson T, Sreenan JM, et al. Amino acids in oviduct and uterine fluid and blood plasma during the estrous cycle in the bovine. Mol Reprod Dev 2007;74:445–54. https://doi.org/10.1002/mrd.20607.

[5] Maloney S, Khan FA, Chenier TS, Diel de Amorim M, Anthony Hayes M, Scholtz EL. A comparison of the uterine proteome of mares in oestrus and dioestrus. Reprod Domest Anim 2019;54:473–9. https://doi.org/10.1111/rda.13375.

[6] Gegenfurtner K, Fröhlich T, Flenkenthaler F, Kösters M, Fritz S, Desnoës O, et al. Genetic merit for fertility alters the bovine uterine luminal fluid proteome. Biol Reprod 2020;102:730–9. https://doi.org/10.1093/biolre/ioz216.

[7] Kasvandik S, Saarma M, Kaart T, Rooda I, Velthut-Meikas A, Ehrenberg A, et al. Uterine fluid proteins for minimally invasive assessment of endometrial receptivity. J Clin Endocrinol Metab 2020;105:219–30. https://doi.org/10.1210/clinem/dgz019.

[8] Abe H, Sendai Y, Satoh T, Hoshi H. Secretory products of bovine oviductal epithelial cells support the viability and motility of bovine spermatozoa in culture in vitro. J Exp Zool 1995;272:54–61. https://doi.org/10.1002/jez.1402720107.

[9] Chirinos M, Durand M, González-González ME, Hernández-Silva G, Maldonado-Rosas I, López P, et al. Uterine flushings from women treated with levonorgestrel affect sperm functionality in vitro. Reprod Camb Engl 2017;154:607–14. https://doi.org/10.1530/REP-17-0313.

[10] Luongo C, Abril-Sánchez S, Hernández JG, García-Vázquez FA. Seminal plasma mitigates the adverse effect of uterine fluid on boar spermatozoa. Theriogenology 2019;136:28–35. https://doi.org/10.1016/j.theriogenology.2019.06.018.

[11] Hamdi M, Lopera-Vasquez R, Maillo V, Sanchez-Calabuig MJ, Núnez C, Gutierrez-Adan A, et al. Bovine oviductal and uterine fluid support in vitro embryo development. Reprod Fertil Dev 2018;30:935. https://doi.org/10.1071/RD17286.

[12] Lee RK-K, Tseng H-C, Hwu Y-M, Fan C-C, Lin M-H, Yu J-J, et al. Expression of cystatin C in the female reproductive tract and its effect on human sperm capacitation. Reprod Biol Endocrinol 2018;16:8. https://doi.org/10.1186/s12958-018-0327-0.

[13] Banliat C, Tsikis G, Labas V, Teixeira-Gomes A-P, Com E, Lavigne R, et al. Identification of 56 proteins involved in embryo–maternal interactions in the bovine oviduct. Int J Mol Sci 2020;21:466. https://doi.org/10.3390/ijms21020466.
[14] Mahé C, Lavigne R, Com E, Pineau C, Locatelli Y, Zlotkowska AM, et al. Spatiotemporal profiling of the bovine oviduct fluid proteome around the time of ovulation. Sci Rep 2022;12:4135. https://doi.org/10.1038/s41598-022-07929-3.
[15] Khan FA, Diel de Amorim M, Chenier TS. Qualitative analysis and functional classification of the uterine proteome of mares in oestrus and dioestrus. Reprod Domest Anim 2020;55:1511–9. https://doi.org/10.1111/rda.13800.
[16] Soleilhavoup C, Riou C, Tsikis G, Labas V, Harichaux G, Kohnke P, et al. Proteomes of the female genital tract during the oestrous cycle. Mol Cell Proteomics 2016;15:93–108. https://doi.org/10.1074/mcp.M115.052332.
[17] Sánchez JM, Passaro C, Forde N, Browne JA, Behura SK, Fernández-Fuertes B, et al. Do differences in the endometrial transcriptome between uterine horns ipsilateral and contralateral to the corpus luteum influence conceptus growth to day 14 in cattle? Biol Reprod 2019;100:86–100. https://doi.org/10.1093/biolre/ioy185.
[18] Faulkner S, Elia G, O'Boyle P, Dunn M, Morris D. Composition of the bovine uterine proteome is associated with stage of cycle and concentration of systemic progesterone. Proteomics 2013;13:3333–53. https://doi.org/10.1002/pmic.201300204.
[19] Mullen MP, Elia G, Hilliard M, Parr MH, Diskin MG, Evans ACO, et al. Proteomic characterization of histotroph during the preimplantation phase of the estrous cycle in Cattle. J Proteome Res 2012;11:3004–18. https://doi.org/10.1021/pr300144q.
[20] Forde N, McGettigan PA, Mehta JP, O'Hara L, Mamo S, Bazer FW, et al. Proteomic analysis of uterine fluid during the pre-implantation period of pregnancy in cattle. Reproduction 2014;147:575–87. https://doi.org/10.1530/REP-13-0010.
[21] Keller A, Nesvizhskii AI, Kolker E, Aebersold R. Empirical statistical model to estimate the accuracy of peptide identifications made by MS/MS and database search. Anal Chem 2002;74:5383–92. https://doi.org/10.1021/ac025747h.
[22] Nesvizhskii AI, Keller A, Kolker E, Aebersold R. A statistical model for identifying proteins by tandem mass spectrometry. Anal Chem 2003;75:4646–58. https://doi.org/10.1021/ac0341261.
[23] Bardou P, Mariette J, Escudié F, Djemiel C, Klopp C. jvenn: an interactive Venn diagram viewer. BMC Bioinformatics 2014;15:293. https://doi.org/10.1186/1471-2105-15-293.
[24] Zhao L, Poschmann G, Waldera-Lupa D, Rafiee N, Kollmann M, Stühler K. OutCyte: a novel tool for predicting unconventional protein secretion. Sci Rep 2019;9:19448. https://doi.org/10.1038/s41598-019-55351-z.
[25] Teufel F, Almagro Armenteros JJ, Johansen AR, Gíslason MH, Pihl SI, Tsirigos KD, et al. SignalP 6.0 predicts all five types of signal peptides using protein language models. Nat Biotechnol 2022;40:1023–5. https://doi.org/10.1038/s41587-021-01156-3.
[26] Kusama K, Nakamura K, Bai R, Nagaoka K, Sakurai T, Imakawa K. Intrauterine exosomes are required for bovine conceptus implantation. Biochem Biophys Res Commun 2018;495:1370–5. https://doi.org/10.1016/j.bbrc.2017.11.176.
[27] Zhou Y, Zhou B, Pache L, Chang M, Khodabakhshi AH, Tanaseichuk O, et al. Metascape provides a biologist-oriented resource for the analysis of systems-level datasets. Nat Commun 2019;10:1523. https://doi.org/10.1038/s41467-019-09234-6.
[28] Liebermeister W, Noor E, Flamholz A, Davidi D, Bernhardt J, Milo R. Visual account of protein investment in cellular functions. Proc Natl Acad Sci 2014;111:8488–93. https://doi.org/10.1073/pnas.1314810111.
[29] Moraes JGN, Behura SK, Bishop JV, Hansen TR, Geary TW, Spencer TE. Analysis of

the uterine lumen in fertility-classified heifers: II. Proteins and metabolites. Biol Reprod 2020;102:571–87. https://doi.org/10.1093/biolre/ioz197.
[30] Ehrenwald E, Foote RH, Parks JE. Bovine oviductal fluid components and their potential role in sperm cholesterol efflux. Mol Reprod Dev 1990;25:195–204. https://doi.org/10.1002/mrd.1080250213.
[31] Bernecic NC, Zhang M, Gadella BM, Brouwers JFHM, Jansen JWA, Arkesteijn GJA, et al. BODIPY-cholesterol can be reliably used to monitor cholesterol efflux from capacitating mammalian spermatozoa. Sci Rep 2019;9. https://doi.org/10.1038/s41598-019-45831-7.
[32] Zhao R, Dai H, Arias RJ, De Blas GA, Orta G, Pavarotti MA, et al. Direct activation of the proton channel by albumin leads to human sperm capacitation and sustained release of inflammatory mediators by neutrophils. Nat Commun 2021;12:3855. https://doi.org/10.1038/s41467-021-24145-1.
[33] Baker ME. Albumin's role in steroid hormone action and the origins of vertebrates: is albumin an essential protein? FEBS Lett 1998;439:9–12. https://doi.org/10.1016/S0014-5793(98)01346-5.
[34] Hugentobler SA, Humpherson PG, Leese HJ, Sreenan JM, Morris DG. Energy substrates in bovine oviduct and uterine fluid and blood plasma during the oestrous cycle. Mol Reprod Dev 2008;75:496–503. https://doi.org/10.1002/mrd.20760.
[35] Rodriguez-Martinez H, McKenna D, Weston PG, Whitmore HL, Gustafsson BK. Uterine motility in the cow during the estrous cycle. I. Spontaneous activity. Theriogenology 1987;27:337–48. https://doi.org/10.1016/0093-691X(87)90222-6.
[36] Arai M, Yoshioka S, Tasaki Y, Okuda K. Remodeling of bovine endometrium throughout the estrous cycle. Anim Reprod Sci 2013;142:1–9. https://doi.org/10.1016/j.anireprosci.2013.08.003.
[37] Billhaq DH, Lee S, Lee S. The potential function of endometrial-secreted factors for endometrium remodeling during the estrous cycle. Anim Sci J 2020;91. https://doi.org/10.1111/asj.13333.
[38] Song G, Bailey DW, Dunlap KA, Burghardt RC, Spencer TE, Bazer FW, et al. Cathepsin B, Cathepsin L, and Cystatin C in the Porcine Uterus and Placenta: potential roles in endometrial/placental remodeling and in fluid-phase transport of proteins secreted by uterine epithelia across placental Areolae. Biol Reprod 2010;82:854–64. https://doi.org/10.1095/biolreprod.109.080929.
[39] Song G, Spencer TE, Bazer FW. Cathepsins in the ovine uterus: regulation by pregnancy, progesterone, and interferon tau. Endocrinology 2005;146:4825–33. https://doi.org/10.1210/en.2005-0768.
[40] França MR, da Silva MIS, Pugliesi G, Van Hoeck V, Binelli M. Evidence of endometrial amino acid metabolism and transport modulation by peri-ovulatory endocrine profiles driving uterine receptivity. J Anim Sci Biotechnol 2017;8:54. https://doi.org/10.1186/s40104-017-0185-1.
[41] Williams AC, Ford WC. The role of glucose in supporting motility and capacitation in human spermatozoa. J Androl 2001;22:680–95. https://doi.org/10.1002/j.1939-4640.2001.tb02229.x.
[42] Ferramosca A, Zara V. Bioenergetics of mammalian sperm capacitation. BioMed Res Int 2014;2014:1–8. https://doi.org/10.1155/2014/902953.
[43] Khurana NK, Niemann H. Energy metabolism in preimplantation bovine embryos derived in vitro or in vivo. Biol Reprod 2000;62:847–56. https://doi.org/10.1095/biolreprod62.4.847.
[44] Kim K-U, Pang W-K, Kang S, Ryu D-Y, Song W-H, Rahman MS, et al. Sperm solute carrier family 9 regulator 1 is correlated with boar fertility. Theriogenology 2019;126:254–60.

https://doi.org/10.1016/j.theriogenology.2018.12.023.
[45] Chávez JC, Hernández-González EO, Wertheimer E, Visconti PE, Darszon A, Treviño CL. Participation of the Cl−/HCO3− Exchangers SLC26A3 and SLC26A6, the Cl− Channel CFTR, and the Regulatory Factor SLC9A3R1 in Mouse Sperm Capacitation1. Biol Reprod 2012;86. https://doi.org/10.1095/biolreprod.111.094037.
[46] Ribeiro JC, Braga PC, Martins AD, Silva BM, Alves MG, Oliveira PF. Antioxidants present in reproductive tract fluids and their relevance for fertility. Antioxidants 2021;10:1441. https://doi.org/10.3390/antiox10091441.
[47] Lee D, Moawad AR, Morielli T, Fernandez MC, O'Flaherty C. Peroxiredoxins prevent oxidative stress during human sperm capacitation. Mol Hum Reprod 2016;23:106–15. https://doi.org/10.1093/molehr/gaw081.
[48] Gong S, Gabriel MCS, Zini A, Chan P, O'Flaherty C. Low amounts and high thiol oxidation of peroxiredoxins in spermatozoa from infertile men. J Androl 2012;33:1342–51. https://doi.org/10.2164/jandrol.111.016162.
[49] Bing YZ, Hirao Y, Takenouchi N, Che LM, Nakamura H, Yodoi J, et al. Effects of thioredoxin on the preimplantation development of bovine embryos. Theriogenology 2003;59:863–73. https://doi.org/10.1016/S0093-691X(02)01158-5.
[50] Majewski P, Majchrzak-Gorecka M, Grygier B, Skrzeczynska-Moncznik J, Osiecka O, Cichy J. Inhibitors of serine proteases in regulating the production and function of neutrophil extracellular traps. Front Immunol 2016;7. https://doi.org/10.3389/fimmu.2016.00261.
[51] Farley K, Stolley JM, Zhao P, Cooley J, Remold-O'Donnell E. A serpinB1 regulatory mechanism is essential for restricting neutrophil extracellular trap generation. J Immunol Baltim Md 1950 2012;189:4574–81. https://doi.org/10.4049/jimmunol.1201167.
[52] Moya C, Rivera-Concha R, Pezo F, Uribe P, Schulz M, Sánchez R, et al. Adverse effects of single neutrophil extracellular trap-derived components on bovine sperm function. Animals 2022;12:1308. https://doi.org/10.3390/ani12101308.
[53] Chaney HL, Grose LF, LaBarbara JM, Sirk AW, Blancke AM, Sánchez JM, et al. Galectin-1 induces gene and protein expression related to maternal-conceptus immune tolerance in bovine endometrium. Biol Reprod 2022;106:487–502. https://doi.org/10.1093/biolre/ioab215.
[54] Faulkner S, Elia G, Mullen MP, O'Boyle P, Dunn MJ, Morris D. A comparison of the bovine uterine and plasma proteome using iTRAQ proteomics. PROTEOMICS 2012;12:2014–23. https://doi.org/10.1002/pmic.201100609.
[55] Fair T. The contribution of the maternal immune system to the establishment of pregnancy in cattle. Front Immunol 2015;6. https://doi.org/10.3389/fimmu.2015.00007.
[56] Wrenzycki C. Interaction of sperm cells with the female reproductive tract in cattle: Focus on neutrophil extracellular trap formation. Anim Reprod Sci 2022:107056. https://doi.org/10.1016/j.anireprosci.2022.107056.
[57] Weber KS, Wagener K, Blanco M, Bauersachs S, Bollwein H. A comparative analysis of the intrauterine transcriptome in fertile and subfertile mares using cytobrush sampling. BMC Genomics 2021;22:377. https://doi.org/10.1186/s12864-021-07701-3.
[58] Qu X, Han Y, Chen X, Lv Y, Zhang Y, Cao L, et al. Inhibition of 26 S proteasome enhances AKAP3-mediated cAMP-PKA signaling during boar sperm capacitation. Anim Reprod Sci 2022:107079. https://doi.org/10.1016/j.anireprosci.2022.107079.
[59] Smits K, Willems S, Van Steendam K, Van De Velde M, De Lange V, Ververs C, et al. Proteins involved in embryo-maternal interaction around the signalling of maternal recognition of pregnancy in the horse. Sci Rep 2018;8:5249. https://doi.org/10.1038/s41598-018-23537-6.
[60] Mahé C, Lavigne R, Com E, Pineau C, Zlotkowska AM, Guillaume T, et al. The

sperm-interacting proteome in bovine oviduct fluid: temporal and spatial resolution. In Review; 2022. https://doi.org/10.21203/rs.3.rs-1854650/v1.
[61] Almiñana C, Rudolf Vegas A, Tekin M, Hassan M, Uzbekov R, Fröhlich T, et al. Isolation and characterization of equine uterine extracellular vesicles: a comparative methodological study. Int J Mol Sci 2021;22:979. https://doi.org/10.3390/ijms22020979.
[62] Hamdi M, Cañon-Beltrán K, Mazzarella R, Cajas YN, Leal CLV, Gutierrez-Adan A, et al. Characterization and profiling analysis of bovine oviduct and uterine extracellular vesicles and their miRNA cargo through the estrous cycle. FASEB J 2021;35:e22000. https://doi.org/10.1096/fj.202101023R.
[63] Griffiths GS, Galileo DS, Reese K, Martin-DeLeon PA. Investigating the role of murine epididymosomes and uterosomes in GPI-linked protein transfer to sperm using SPAM1 as a model. Mol Reprod Dev 2008;75:1627–36. https://doi.org/10.1002/mrd.20907.
[64] Franchi A, Cubilla M, Guidobaldi HA, Bravo AA, Giojalas LC. Uterosome-like vesicles prompt human sperm fertilizing capability. Mol Hum Reprod 2016:molehr;gaw066v2. https://doi.org/10.1093/molehr/gaw066.
[65] Burns GW, Brooks KE, Spencer TE. Extracellular vesicles originate from the conceptus and uterus during early pregnancy in sheep. Biol Reprod 2016;94. https://doi.org/10.1095/biolreprod.115.134973.
[66] Lamy J, Labas V, Harichaux G, Tsikis G, Mermillod P, Saint-Dizier M. Regulation of the bovine oviductal fluid proteome. Reproduction 2016;152:629–44. https://doi.org/10.1530/REP-16-0397.
[67] Deutsch EW, Bandeira N, Sharma V, Perez-Riverol Y, Carver JJ, Kundu DJ, et al. The ProteomeXchange consortium in 2020: enabling 'big data' approaches in proteomics. Nucleic Acids Res 2019:gkz984. https://doi.org/10.1093/nar/gkz984.
[68] Perez-Riverol Y, Csordas A, Bai J, Bernal-Llinares M, Hewapathirana S, Kundu DJ, et al. The PRIDE database and related tools and resources in 2019: improving support for quantification data. Nucleic Acids Res 2019;47:D442–50. https://doi.org/10.1093/nar/gky1106.

Figure legends

Fig 1. Distribution of proteins identified in the bovine uterine fluid. Numbers of proteins identified in each uterine horn (ipsilateral vs. contralateral to ovulation) at each stage (pre-ovulatory vs. post-ovulatory) are indicated in the histogram.

Fig. 2. Distribution of proteins in the bovine uterine fluid according to their secretory pathways. Classical and unconventional secretion pathways were predicted using the Outcyte and SignalP online tools. Proteins previously reported in bovine UF-derived extracellular vesicles [26] are also indicated.

Fig. 3. Top-15 most abundant proteins quantified in the bovine uterine fluid. Data are expressed as means ± SEM of biological replicates.

Fig. 4. Principal component analysis of quantified proteins in all samples. Each spot represents one biological replicate and the colored squares represent the means of data in a given condition.

Fig. 5. Differentially abundant proteins between ipsilateral and contralateral uterine horns at pre-ovulatory (A) and post-ovulatory (B) stages of cycle. Protein names in pink were associated with the gene ontology terms containing "reproduction" (RUVBL1, WFDC2), "sperm" (RUVBL1), or "embryo" (TUBB2B), as indicated in frames. See Table S4 for the complete list of GO terms with corresponding gene symbols.

Fig. 6. **Differentially abundant proteins between pre- and post-ovulatory stages of cycle in the uterine horns ipsilateral (A) and contralateral (B) to ovulation**. Protein names in pink were associated with the gene ontology terms containing "reproduction" (FOLR1, HSPA5, PAFAH1B3, RUVBL1), "sperm" (FOLR1, PAFAH1B3, RUVBL1), or "embryo" (FOLR1, MTHFD1, SLC9A3R1, TUBB2B), as indicated in frames. See Table S4 for the complete list of GO terms with corresponding gene symbols.

Fig. 7. Functional enrichment analysis of proteins identified in the uterine fluid. The Metascape bar graphs represent the top 20 clusters of enriched gene ontology terms for molecular functions (A), biological processes (B), and cellular components (C). Each row represents one enriched cluster, and the darker color of the bars indicates higher significance (lower *P*-value). See Table S3 for the complete list of GO terms with corresponding gene symbols and p-values.

Fig. 8. Proteomaps of differentially abundant proteins between pre- and post-ovulatory stages of cycle in the uterine horn ipsilateral to ovulation. Each panel was built by the Proteomaps online tool. Each protein is shown by a polygon (A) and functionally related proteins are arranged in common regions based on the KEGG Pathways gene classification (B, and C). Polygon areas represent the mean abundance at the pre-ovulatory stage of cycle.

1,214 identified proteins in the bovine uterine fluid

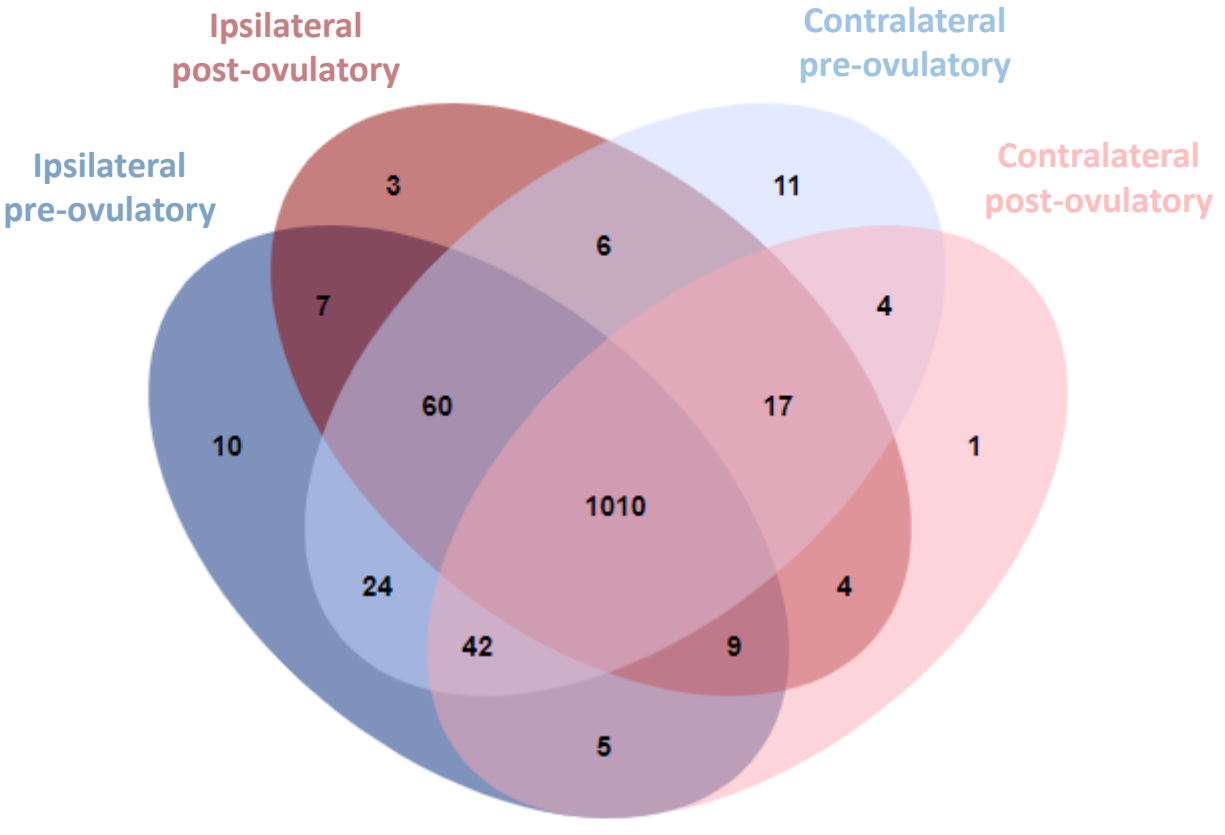

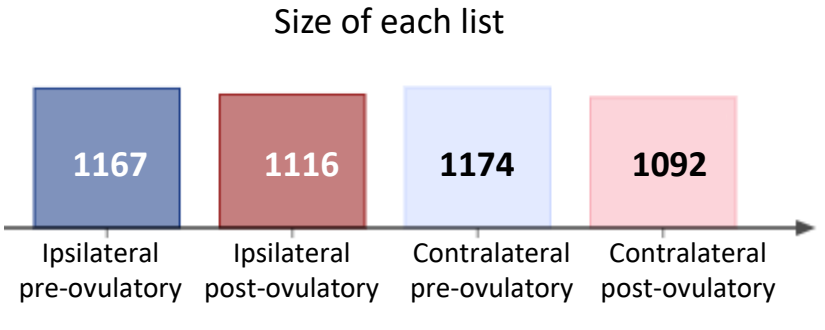

17 % (204/1214) previously reported in **bovine uterine fluid derived extracellular vesicles**

20 % (243/1,214) of proteins contained a **signal peptide** and were predicted to be classically secreted

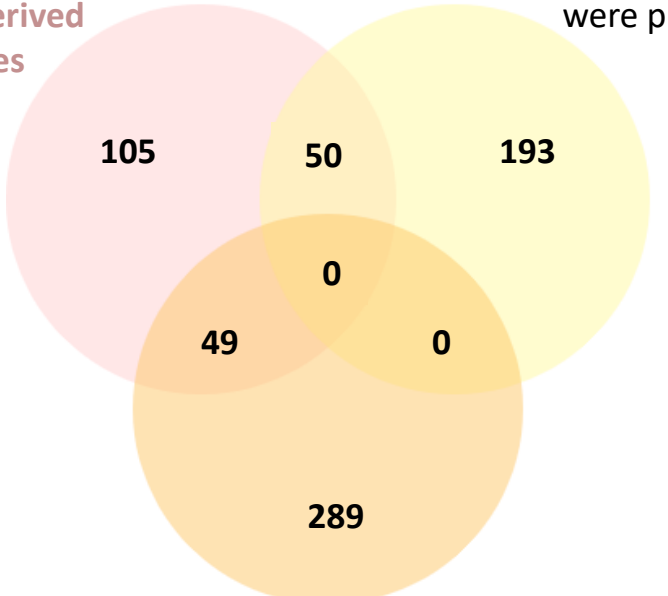

28% (338/1,214) of **unconventionnaly secreted proteins**

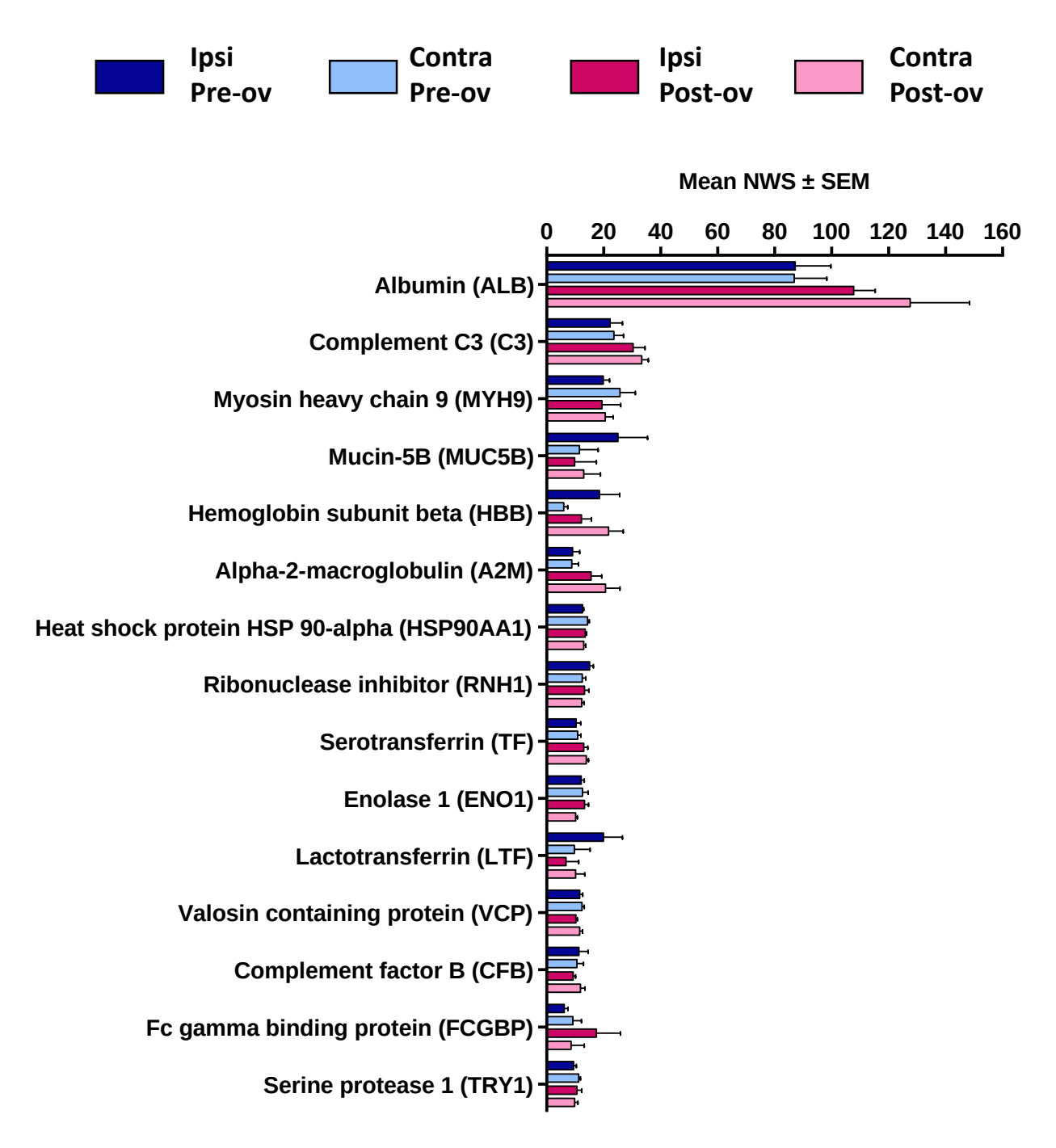
Ipsi Pre-ov
Contra Pre-ov
Ipsi Post-ov
Contra Post-ov
Mean NWS ± SEM
0
20
40
60
80
100
120
140
160
Albumin (ALB)
Complement C3 (C3)
Myosin heavy chain 9 (MYH9)
Mucin-5B (MUC5B)
Hemoglobin subunit beta (HBB)
Alpha-2-macroglobulin (A2M)
Heat shock protein HSP 90-alpha (HSP90AA1)
Ribonuclease inhibitor (RNH1)
Serotransferrin (TF)
Enolase 1 (ENO1)
Lactotransferrin (LTF)
Valosin containing protein (VCP)
Complement factor B (CFB)
Fc gamma binding protein (FCGBP)
Serine protease 1 (TRY1)

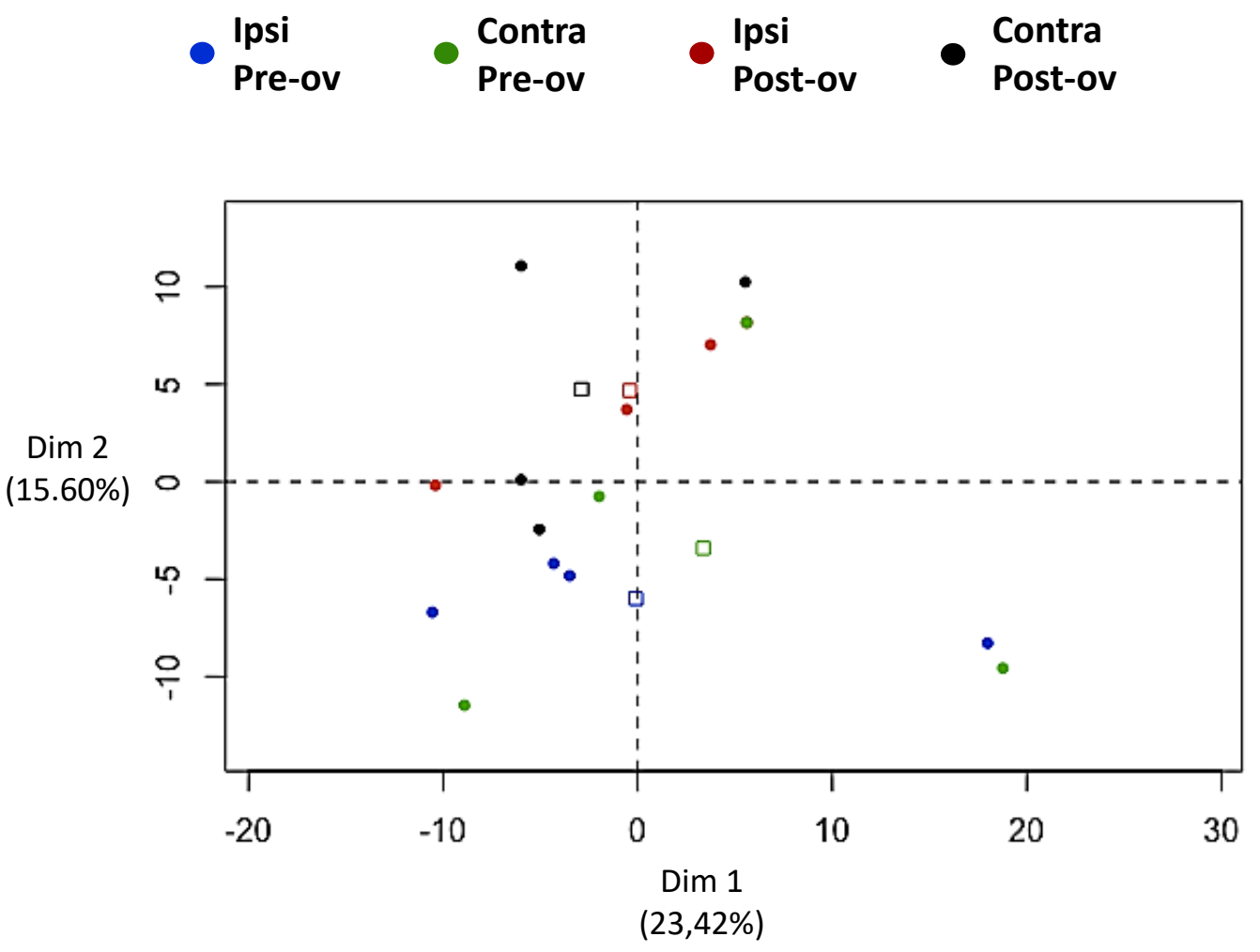
Ipsi Pre-ov
Contra Pre-ov
Ipsi Post-ov
Contra Post-ov
Dim 2 (15.60%)
10
5
0
-5
-10
-20
-10
0
10
20
30
Dim 1 (23,42%)

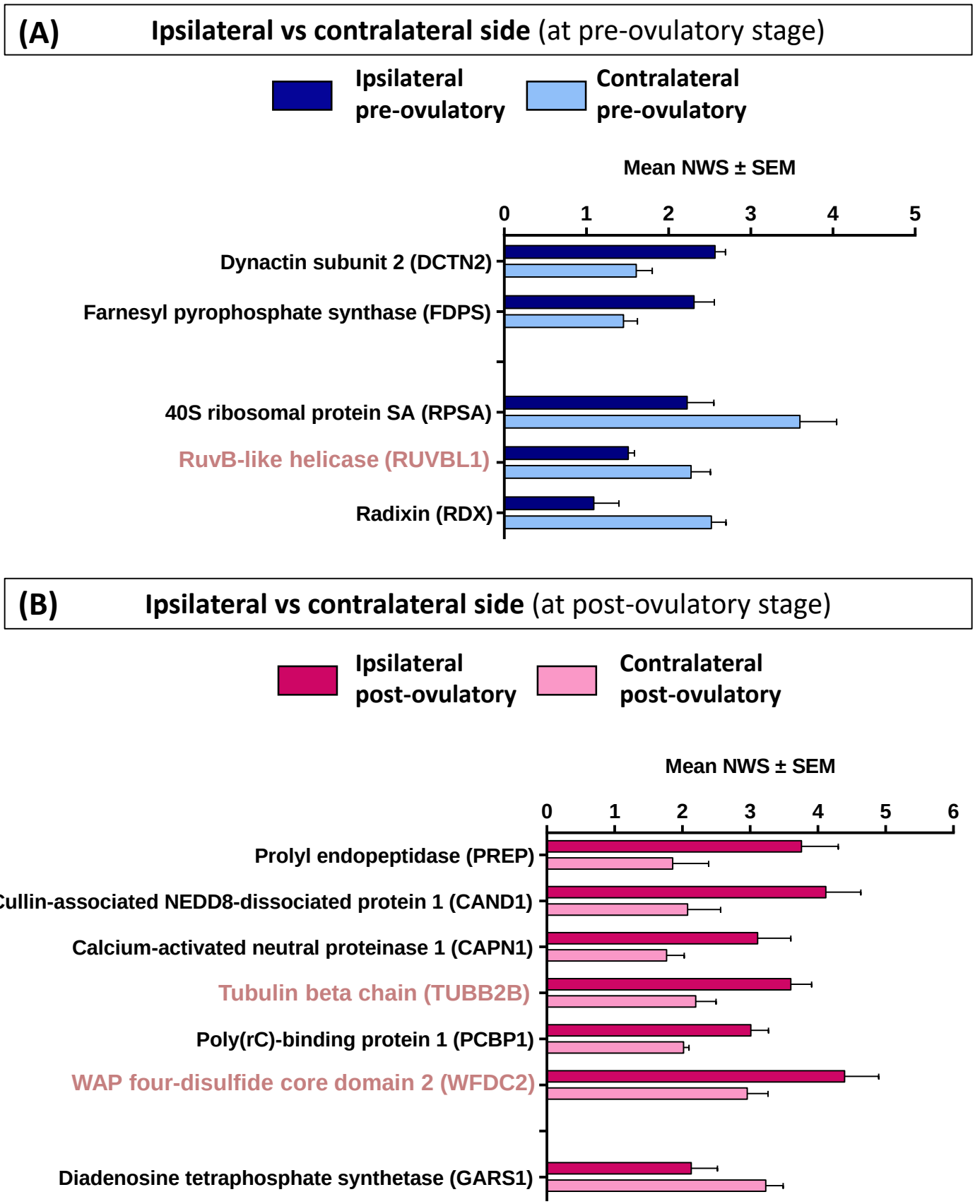
(A) Ipsilateral vs contralateral side (at pre-ovulatory stage)
Ipsilateral pre-ovulatory
Contralateral pre-ovulatory
Mean NWS ± SEM
0
1
2
3
4
5
Dynactin subunit 2 (DCTN2)
Farnesyl pyrophosphate synthase (FDPS)
40S ribosomal protein SA (RPSA)
RuvB-like helicase (RUVBL1)
Radixin (RDX)
(B) Ipsilateral vs contralateral side (at post-ovulatory stage)
Ipsilateral post-ovulatory
Contralateral post-ovulatory
Mean NWS ± SEM
0
1
2
3
4
5
6
Prolyl endopeptidase (PREP)
Cullin-associated NEDD8-dissociated protein 1 (CAND1)
Calcium-activated neutral proteinase 1 (CAPN1)
Tubulin beta chain (TUBB2B)
Poly(rC)-binding protein 1 (PCBP1)
WAP four-disulfide core domain 2 (WFDC2)
Diadenosine tetraphosphate synthetase (GARS1)

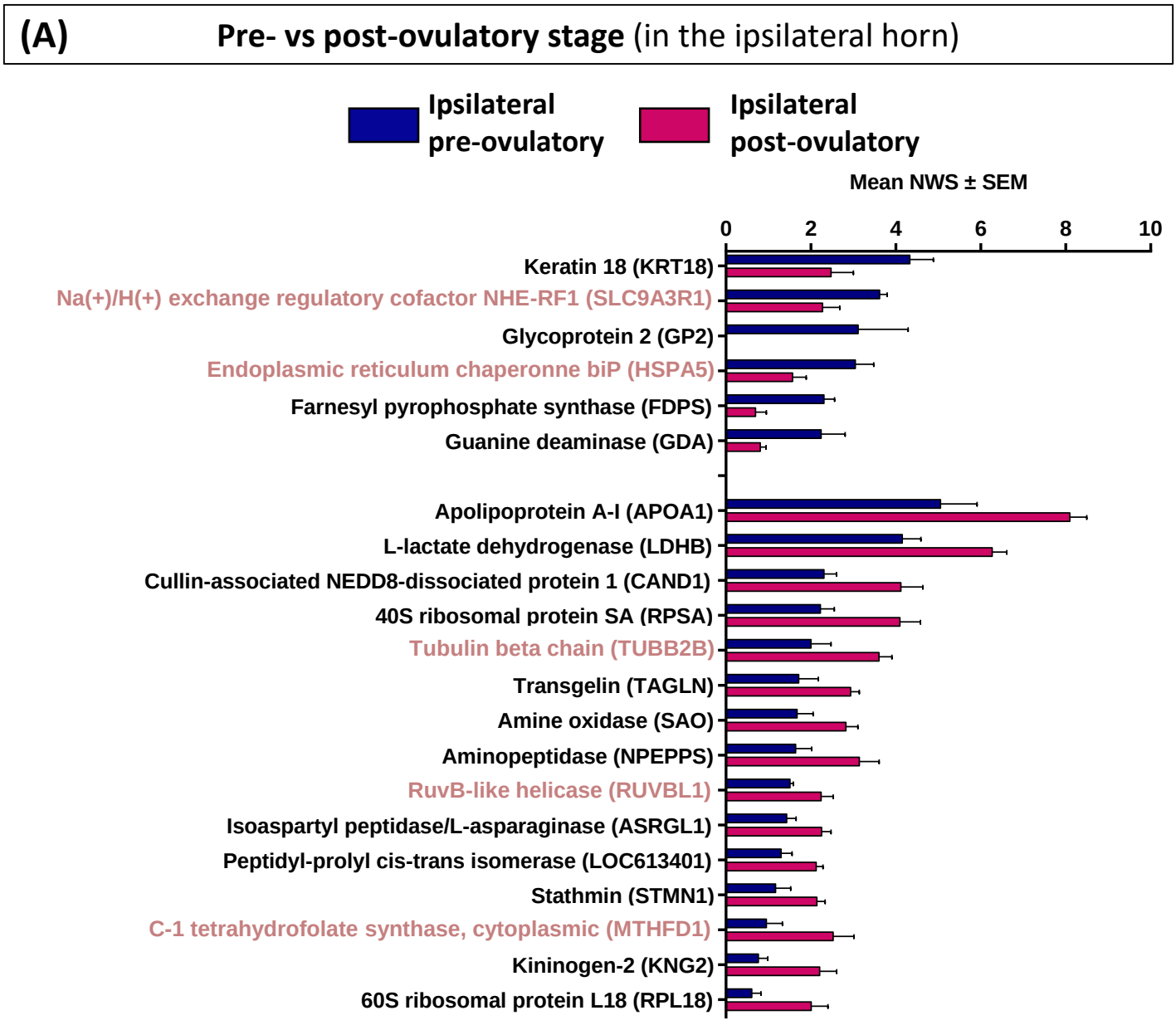
(A) Pre- vs post-ovulatory stage (in the ipsilateral horn)
Ipsilateral pre-ovulatory
Ipsilateral post-ovulatory
Mean NWS ± SEM
0
2
4
6
8
10
Keratin 18 (KRT18)
Na(+)/H(+) exchange regulatory cofactor NHE-RF1 (SLC9A3R1)
Glycoprotein 2 (GP2)
Endoplasmic reticulum chaperonne biP (HSPA5)
Farnesyl pyrophosphate synthase (FDPS)
Guanine deaminase (GDA)
Apolipoprotein A-I (APOA1)
L-lactate dehydrogenase (LDHB)
Cullin-associated NEDD8-dissociated protein 1 (CAND1)
40S ribosomal protein SA (RPSA)
Tubulin beta chain (TUBB2B)
Transgelin (TAGLN)
Amine oxidase (SAO)
Aminopeptidase (NPEPPS)
RuvB-like helicase (RUVBL1)
Isoaspartyl peptidase/L-asparaginase (ASRGL1)
Peptidyl-prolyl cis-trans isomerase (LOC613401)
Stathmin (STMN1)
C-1 tetrahydrofolate synthase, cytoplasmic (MTHFD1)
Kininogen-2 (KNG2)
60S ribosomal protein L18 (RPL18)

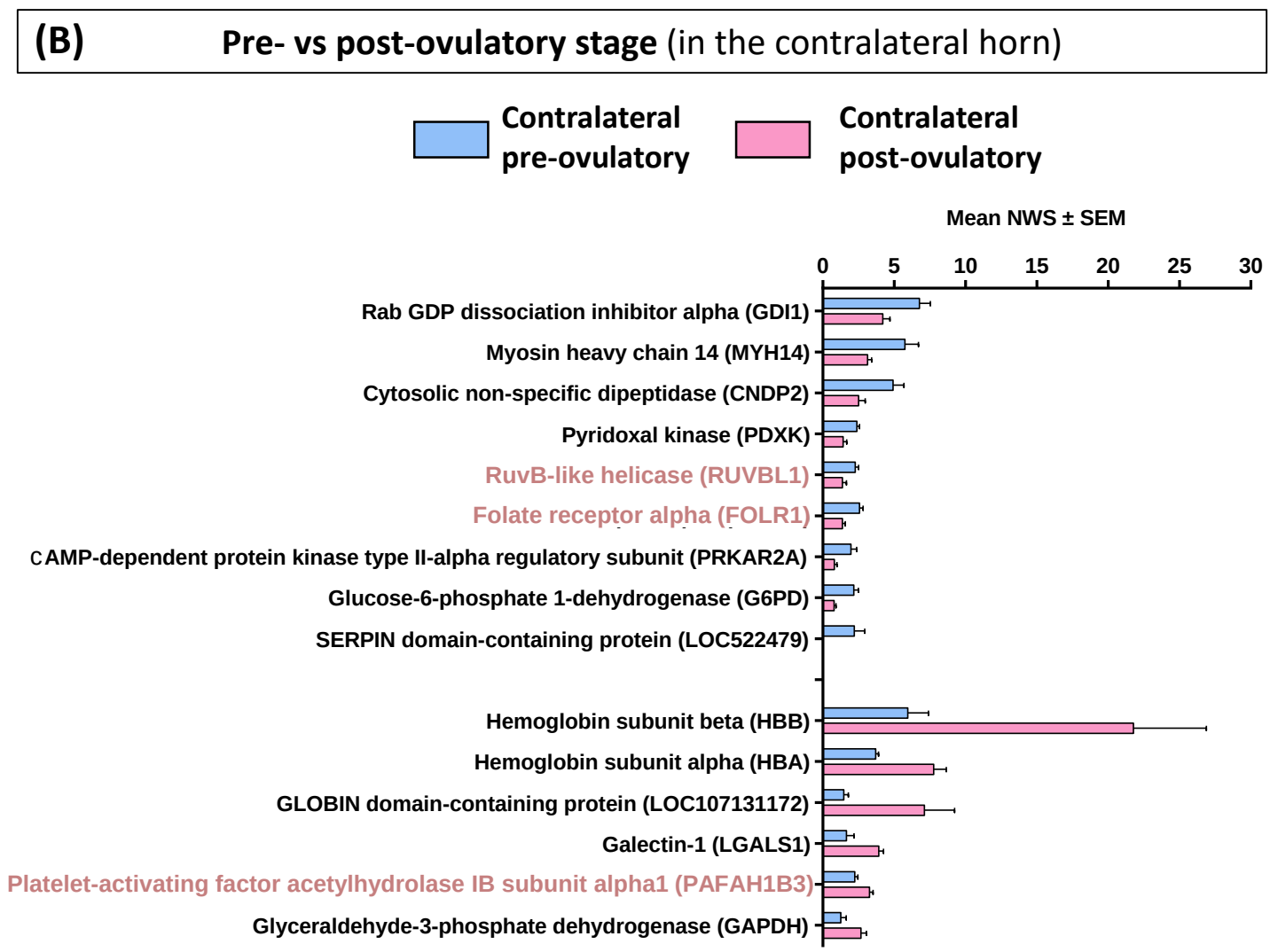
(B) Pre- vs post-ovulatory stage (in the contralateral horn)
Contralateral pre-ovulatory
Contralateral post-ovulatory
Mean NWS ± SEM
0
5
10
15
20
25
30
Rab GDP dissociation inhibitor alpha (GDI1)
Myosin heavy chain 14 (MYH14)
Cytosolic non-specific dipeptidase (CNDP2)
Pyridoxal kinase (PDXK)
RuvB-like helicase (RUVBL1)
Folate receptor alpha (FOLR1)
cAMP-dependent protein kinase type II-alpha regulatory subunit (PRKAR2A)
Glucose-6-phosphate 1-dehydrogenase (G6PD)
SERPIN domain-containing protein (LOC522479)
Hemoglobin subunit beta (HBB)
Hemoglobin subunit alpha (HBA)
GLOBIN domain-containing protein (LOC107131172)
Galectin-1 (LGALS1)
Platelet-activating factor acetylhydrolase IB subunit alpha1 (PAFAH1B3)
Glyceraldehyde-3-phosphate dehydrogenase (GAPDH)

(A) Gene ontology molecular functions

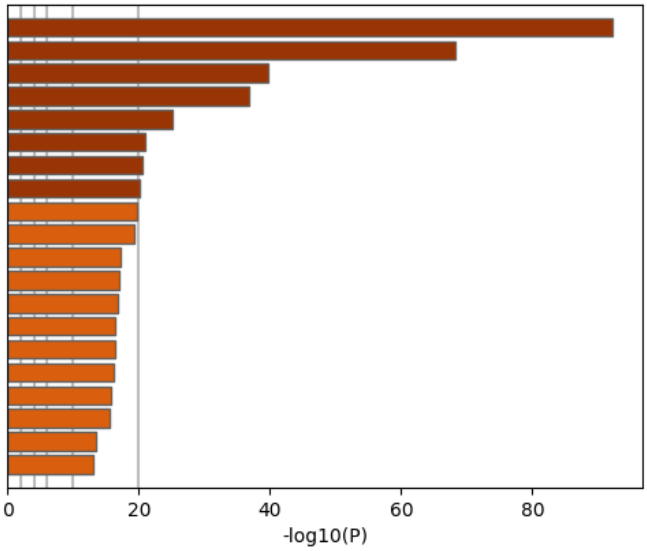

GO:0045296: cadherin binding
GO:0005198: structural molecule activity
GO:0003779: actin binding
GO:0004857: enzyme inhibitor activity
GO:0042803: protein homodimerization activity
GO:0003735: structural constituent of ribosome
GO:0016462: pyrophosphatase activity
GO:0051082: unfolded protein binding
GO:0019904: protein domain specific binding
GO:0016874: ligase activity
GO:0051020: GTPase binding
GO:0008233: peptidase activity
GO:0008135: translation factor activity, RNA binding
GO:0031625: ubiquitin protein ligase binding
GO:0008289: lipid binding
GO:0016491: oxidoreductase activity
GO:0019901: protein kinase binding
GO:0016209: antioxidant activity
GO:0005201: extracellular matrix structural constituent
GO:0005509: calcium ion binding

(B) Gene ontology biological processes

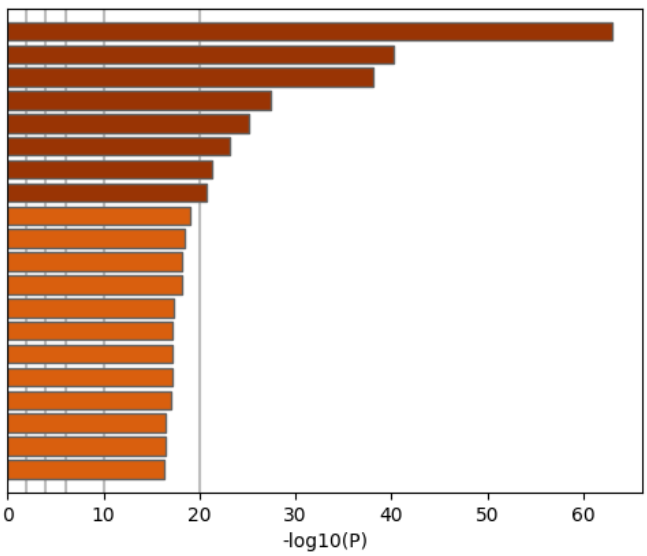

GO:0006518: peptide metabolic process
GO:0030036: actin cytoskeleton organization
GO:0043086: negative regulation of catalytic activity
GO:0055086: nucleobase-containing small molecule metabolic process
GO:0005975: carbohydrate metabolic process
GO:0006457: protein folding
GO:1990748: cellular detoxification
GO:0006520: cellular amino acid metabolic process
GO:0006418: tRNA aminoacylation for protein translation
GO:0010638: positive regulation of organelle organization
GO:0030163: protein catabolic process
GO:0022604: regulation of cell morphogenesis
GO:0009611: response to wounding
GO:0042176: regulation of protein catabolic process
GO:0006413: translational initiation
GO:0031400: negative regulation of protein modification process
GO:0006886: intracellular protein transport
GO:0010035: response to inorganic substance
GO:0034248: regulation of cellular amide metabolic process
GO:0060341: regulation of cellular localization

(C) Gene ontology cellular component

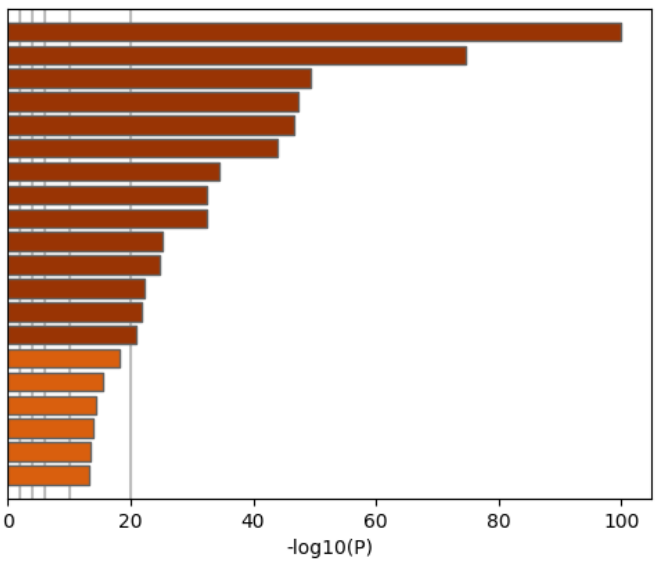

GO:0034774: secretory granule lumen
GO:0005925: focal adhesion
GO:0005775: vacuolar lumen
GO:0072562: blood microparticle
GO:0062023: collagen-containing extracellular matrix
GO:0015629: actin cytoskeleton
GO:0000502: proteasome complex
GO:0099513: polymeric cytoskeletal fiber
GO:0022626: cytosolic ribosome
GO:0031252: cell leading edge
GO:0048471: perinuclear region of cytoplasm
GO:1904724: tertiary granule lumen
GO:0042470: melanosome
GO:0031093: platelet alpha granule lumen
GO:0101031: chaperone complex
GO:0005911: cell-cell junction
GO:0032432: actin filament bundle
GO:0036464: cytoplasmic ribonucleoprotein granule
GO:0005903: brush border
GO:0017101: aminoacyl-tRNA synthetase multienzyme complex

(A)

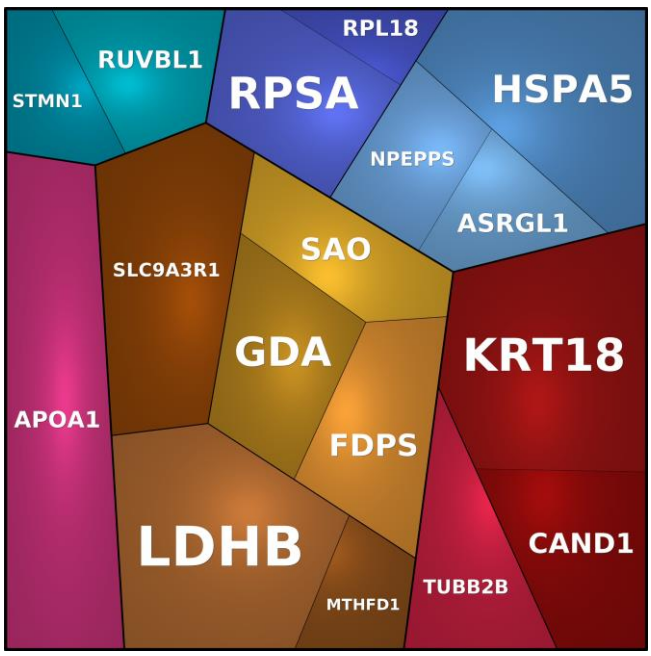
RPL18
RUVBL1
STMN1
RPSA
HSPA5
NPEPPS
ASRGL1
SAO
SLC9A3R1
GDA
KRT18
APOA1
FDPS
LDHB
CAND1
TUBB2B
MTHFD1

(B)

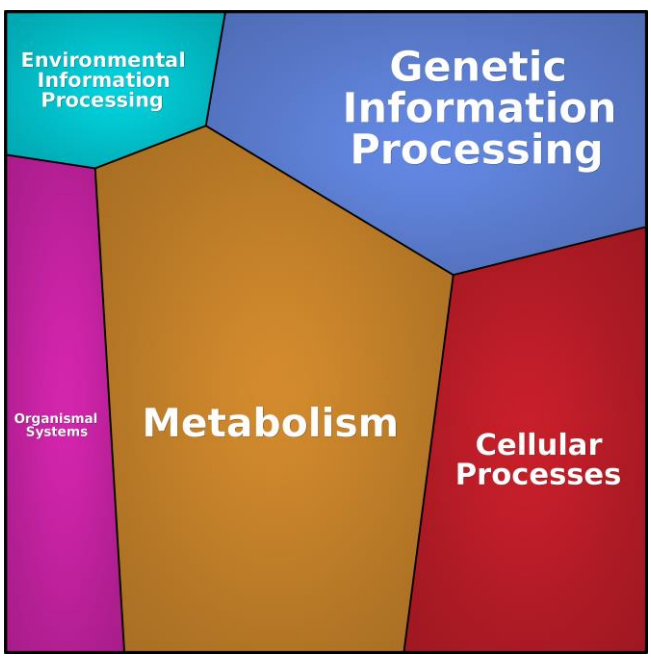
Environmental Information Processing
Genetic Information Processing
Organismal Systems
Metabolism
Cellular Processes

(C)

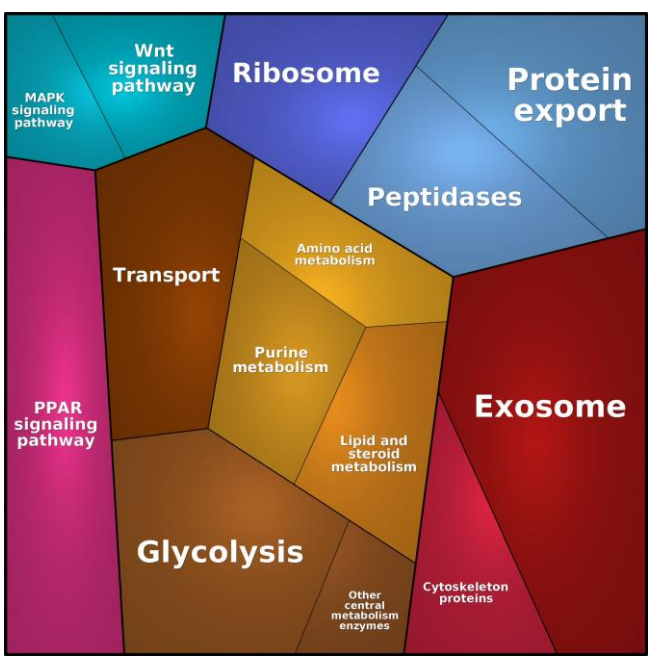
Wnt signaling pathway
MAPK signaling pathway
Ribosome
Protein export
Peptidases
Amino acid metabolism
Transport
Purine metabolism
PPAR signaling pathway
Exosome
Lipid and steroid metabolism
Glycolysis
Other central metabolism enzymes
Cytoskeleton proteins